ORIGINAL ARTICLE

Protease-armed, Pathogenic Extracellular Vesicles Link Smoking and Chronic Obstructive Pulmonary Disease

Matthew C. Madison[1]*, Camilla Margaroli[2]*, Kristopher R. Genschmer[3,4], Derek W. Russell[3,4,5,6], James M. Wells[3,4,5,6], Ezgi Sari[3], Yixel M. Soto-Vazquez[3], Yuan-Yuan Guo[6], Kyle T. Mincham[7], Robert J. Snelgrove[7], Amit Gaggar[3,4,5,6], and James E. Blalock[3,4,5]

[1]Department of Clinical and Diagnostic Science, [2]Department of Pathology, [3]Division of Pulmonary, Allergy & Critical Care Medicine, Department of Medicine, [4]Program in Protease and Matrix Biology, and [5]Lung Health Center and Gregory Fleming James CF Center, University of Alabama at Birmingham, Birmingham, Alabama; [6]Birmingham VA Medical Center, Birmingham, Alabama; and [7]National Heart and Lung Institute, Imperial College London, London, United Kingdom

ORCID IDs: 0000-0001-8143-7471 (M.C.M.); 0000-0003-3952-0778 (C.M.); 0000-0001-9612-5454 (J.M.W.).

Abstract

Rationale: Mounting evidence demonstrates a role for extracellular vesicles (EVs) in driving lung disorders, such as chronic obstructive pulmonary disease (COPD). Although cigarette smoke (CS) is the primary risk factor for COPD, a link between CS and the EVs that could lead to COPD is unknown.

Objective: To ascertain whether exposure to CS elicits a proteolytic EV signature capable of driving disease pathogenesis.

Methods: Protease expression and enzymatic activity were measured in EVs harvested from the BAL fluid of smoke-exposed mice and otherwise healthy human smokers. Pathogenicity of EVs was examined using pathological tissue scoring after EV transfer into naive recipient mice.

Measurements and Main Results: The analyses revealed a unique EV profile defined by neutrophil- and macrophage-derived EVs. These EVs are characterized by abundant surface expression of neutrophil elastase (NE) and matrix metalloproteinase 12 (MMP12), respectively. CS-induced mouse or human-derived airway EVs had a robust capacity to elicit rapid lung damage in naive recipient mice, with an additive effect of NE- and MMP12-expressing EVs.

Conclusions: These studies demonstrate the capacity of CS to drive the generation of unique EV populations containing NE and MMP12. The coordinated action of these EVs is completely sufficient to drive emphysematous disease, and their presence could operate as a prognostic indicator for COPD development. Furthermore, given the robust capacity of these EVs to elicit emphysema in naive mice, they provide a novel model to facilitate preclinical COPD research. Indeed, the development of this model has led to the discovery of a previously unrecognized CS-induced protective mechanism against EV-mediated damage.

Keywords: COPD; EVs; protease; macrophage; neutrophil

(Received in original form March 14, 2023; accepted in final form September 15, 2023)

*These authors contributed equally to this work.

Supported by NHLBI grants R35HL135710 and R35HL166433 (to J.E.B.); National Institute of General Medical Science grant K12GM088010 (to M.C.M.); NHLBI grants K08HL148514 (to D.W.R.), R01HL102371 (to A.G.), and R01HL153113 (to A.G.); US Veterans Affairs Administration (VA MERIT Review) grant I01CX001969 (to A.G.); NHLBI grants R01HL162705 (to K.R.G.) and R01HL148215 (to J.M.W.); Cystic Fibrosis Foundation Research Development Program grant ROWE19R0 (to C.M.); NIH/NHLBI grants R01HL102371 and RO1 HL153113 (to A.G.); and Veterans Affairs Merit grant 101CX001969 (to A.G.). The authors also acknowledge financial support from Imperial College London through an Imperial College Research Fellowship grant awarded to K.T.M. R.J.S. is a Wellcome Trust Senior Research Fellowship in Basic Biomedical Sciences (209458/Z/17/Z). Parts of this work were also funded through a Rosetrees Trust/The Stoneygate Trust project grant (PGS21/10072).

Author Contributions: Conceptualization: M.C.M., C.M., A.G., and J.E.B. Resources: R.J.S., D.W.R., and J.M.W. Investigation: M.C.M., C.M., Y.-Y.G., Y.M.S.-V., E.S., K.R.G., D.W.R., J.M.W., R.J.S., and K.T.M. Funding acquisition: A.G. and J.E.B. Supervision: J.E.B. Writing – original draft: M.C.M. Writing – review and editing: M.C.M., C.M., A.G., J.M.W., and J.E.B.

Correspondence and requests for reprints should be addressed to James E. Blalock, Ph.D., 845 19th Street South, BBRB 834, Birmingham, AL 35294-0005. E-mail: jeblalock@uabmc.edu.

This article has a related editorial.

This article has an online supplement, which is accessible from this issue's table of contents at www.atsjournals.org.

Am J Respir Crit Care Med Vol 208, Iss 10, pp 1115–1125, Nov 15, 2023

Originally Published in Press as DOI: 10.1164/rccm.202303-0471OC on September 15, 2023
Internet address: www.atsjournals.org

At a Glance Commentary

Scientific Knowledge on the Subject: Although extracellular vesicles (EVs) have a variety of homeostatic functions, increasing evidence suggests a role for these membrane-bound vesicles in critical disease processes, including those related to lung disease. EVs harvested from the airways of patients with chronic obstructive pulmonary disease (COPD) exhibit marked protease expression, the capacity to elicit alveolar enlargement, and a resistance to local tissue antiproteases. Although cigarette smoking is a primary risk factor for the development of COPD, the role that it plays in the generation of such pathogenic airway EVs has been unclear.

What This Study Adds to the Field: This work is the first, to our knowledge, to demonstrate that smoke alone elicits an EV signature–bearing neutrophil elastase and matrix metalloprotease 12 with the capacity to induce a COPD-like phenotype, thus directly linking cigarette smoking with disease. Our study also emphasizes EV-associated matrix metalloprotease 12 in the airway, a previously unknown pathogenic mechanism. Moreover, through these studies, we have created a novel animal model to recapitulate the matrix degradation associated with COPD in a rapid fashion.

Pulmonary diseases associated with the use of tobacco products remain a global healthcare burden (1, 2), and mounting evidence demonstrates a role for extracellular vesicles (EVs) in driving lung disease (3–10). Cigarette smoking (CS) is the primary risk factor for the development of chronic obstructive pulmonary disease (COPD) (11), leading to epithelial damage and prompting robust chronic inflammation characterized by continual recruitment of inflammatory cells (e.g., neutrophils and macrophages) into the airways (12–19). These cells, by means of proteases, can degrade the lung's extracellular matrix (ECM) proteins, ultimately causing emphysema and impaired lung function (20–23). We previously discovered that one such protease—neutrophil elastase (NE)—can exist in association with the surface of EVs, and this EV-associated form can cause notable alveolar enlargement and diminished airway physiology (3). Despite these neutrophil-derived, NE-positive EVs having a role in COPD (3), a link between CS exposure and this or any other EV signature is lacking. Furthermore, in the earlier human COPD studies, there was an additional unknown pathogenic EV population also contributing to the phenotype (3). Guided by the rationale and hypotheses outlined (*see* Figure E1 in the online supplement), we sought to develop an animal model of both CS exposure and EV transfer that would enable us to *1*) test whether CS exposure alters EVs in the airway, *2*) characterize the protease burden of CS EVs, and *3*) determine whether the transfer of CS EVs can induce lung damage in naive recipients.

Our studies demonstrate that CS is capable of driving the development of these NE-positive EVs, thus creating a link between CS, EVs, and disease pathology. Moreover, the development of this novel mouse model of CS-activated EV transfer has uncovered a CS-induced protective mechanism, as well as a new pathogenic EV armed with matrix metalloproteinase 12 (MMP12), a protease that is strongly linked to COPD (24–26), which acts in concert with NE-positive EVs to drive emphysematous disease. These two pathogenic EV populations arise early during the course of CS exposure and before observable disease in CS-exposed donors. Such EVs, on their own, recapitulate a number of the clinically relevant changes associated with COPD. Together, our findings highlight CS-induced pathogenic EVs as therapeutic targets and potential prognostic biomarkers for COPD development in smokers.

Methods

Animal Models

Wild-type, A/J, and C57BL/6 mice were purchased from the Jackson Laboratory and housed in the animal resource facility of the University of Alabama at Birmingham. For knockout (KO) experiments, NE-deficient (NEKO) mice (B6.129X1-*Elane*^{tm1Sds}/J) and MMP12-KO mice (B6.129X-Mmp12tm1Sds/J) were purchased from the Jackson Laboratory and housed at the University of Alabama at Birmingham or Imperial College, respectively. Additional details on the animal models and approvals are provided in the online supplement.

Human Sample Collection

Adults from a single center were recruited and categorized into cohorts on the basis of smoking status. Fiberoptic bronchoscopy with airway inspection and BAL was performed using moderate sedation. Additional details on the patient characteristics (Table E1), approvals, and methods for making these measurements are provided in the online supplement.

Mouse Smoke Exposure

For wild-type and NEKO mice in our studies, we implemented a whole-body exposure system (SCIREQ) and the 3R4F research-grade cigarette (University of Kentucky). For studies using MMP12-KO mice, a whole-body cigarette smoke exposure system (Teague Enterprises) was used, which consisted of a time-set pinch valve, exposure chambers, and an extraction unit. In each experiment, five to 10 animals were exposed to either room air or cigarette smoke (from the 3R4F cigarettes) for each respective time point. No animal death resulted from the exposure protocols implemented in this study. Additional details on the exposure methods are provided in the online supplement.

EV Isolation, Characterization, and Transfer

All EVs (mouse and human) used in this study were harvested from BAL fluid (BALF) using differential ultracentrifugation, as previously described (3, 27). Size and EV concentration were determined using the NanoSight N3000 (Malvern Panalytical). EVs were then delivered intratracheally at a single dose of 10^7 EVs per mouse, and the mice were killed 1 week later. Our dosing strategy was guided by our previous studies, which demonstrated that 10^7 EVs was the minimal dose to drive tissue remodeling (27).
For studies analyzing multiple EV doses, three doses of 10^7 EVs per mouse were administered every other day for 1 week. Mice were killed and lungs were harvested 2 days after the final EV dose.

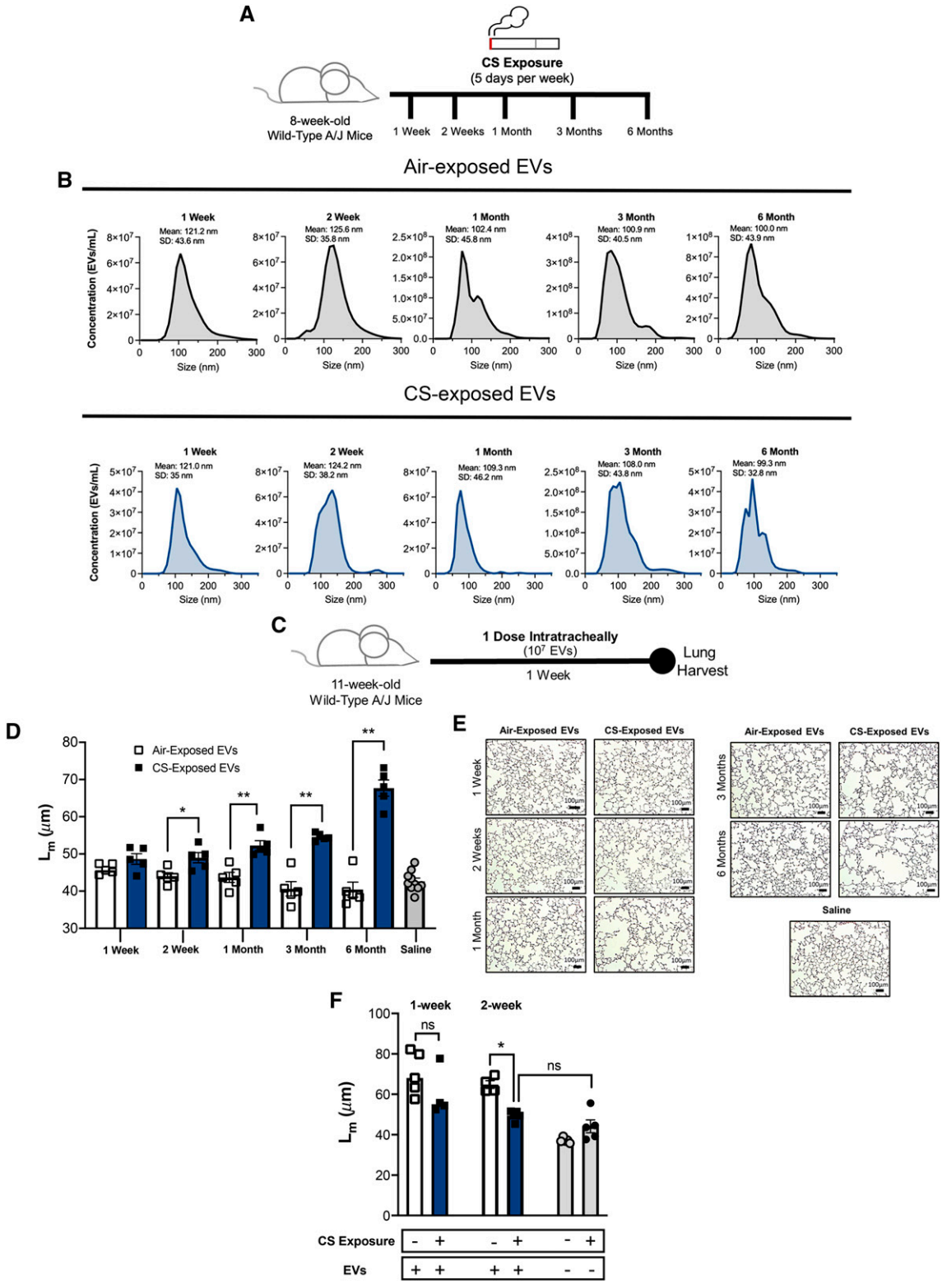

Figure 1. Transfer of cigarette smoking (CS)–exposed extracellular vesicles (EVs) induces alveolar damage in naive recipients. (*A*) Airway EVs from mice receiving cigarette smoke for 1 week, 2 weeks, 1 month, 3 months, or 6 months were harvested, purified, counted. (*B*) Their size distribution was determined using Nanosight NS300. Histograms represent EV samples pooled from five individual mice. Data are representative of two or more independent exposure experiments. (*C*) EVs were transferred to naive A/J mice intratracheally. Mice were treated with one dose (10^7 EVs), and their lung damage was quantified 1 week posttreatment ($n = 5$ per group). (D) Cumulative mean linear intercept (L_m) scoring as a

Cell-Type–Specific EV Depletion

Streptavidin-coated magnetic beads (Spherotech) were washed in ultracentrifuged phosphate-buffered saline (PBS), and 5 μL beads (1% w/v) were incubated with 300 ng biotinylated anti–mouse antibody specific to various cell types for 2 hours on ice; Ly6G for neutrophil-derived EVs (clone 1A8; Miltenyl), CD115 for macrophage-derived EVs (clone AFS98; Miltenyl), and Epcam for epithelium-derived EVs (clone G8.8; Invitrogen). Antibody-coated beads were then washed three times with ultracentrifuged PBS and incubated with 1×10^9 EVs overnight at 4°C on an end-over-end rotating wheel. The next day, beads were removed by means of a magnetic stand, and free EVs were quantified using microfluidics resistive pulse sensing measurements conducted using the nCS1 instrument (Spectradyne). Sample volumes of a few microliters of EVs were diluted 1:10 with 1% polysorbate 20 (Tween 20) in 1 × PBS and loaded onto polydimethylsiloxane cartridges (diameter range, 65–400 nm). Enough events were recorded to achieve less than 5% error for each sample. All results were analyzed with the nCS1 Data Analyzer (Spectradyne).

EV Inhibitor Studies

To assess the contributions of NE and MMP12, in some transfer experiments, EVs were pretreated with NE Inhibitor II (≤50 μM) or an MMP12 inhibitor, MMP408 (≤10 μM). EVs were pretreated with either a single inhibitor or a combination of the two inhibitors for 30 minutes on ice, as previously described (3). After pretreatment, EVs were delivered intratracheally at a single dose of 10^7 EVs per mouse.

Histology and Morphometric Analysis

Lungs were inflated intratracheally and fixed (isobarically) using 10% buffered formalin for 48 hours. Left lungs were selected, paraffin-embedded, sectioned, and stained with hematoxylin and eosin. Lung sections that were stained with hematoxylin and eosin were imaged using the Infinity Analyze 2–1 program. Pathology was assessed by determining the mean linear intercept, as previously described (3, 27).

Enzymatic Activity

To measure the enzymatic activity of both NE and MMP12, we implemented fluorescence resonance energy transfer assays, as described previously (27).

Flow Cytometry

Airway cells obtained from the BAL were stained and measured on the BD FACS Symphony according to methods implemented in previous studies (27). Expression of EV surface proteins was measured using bead-EV conjugates, as previously described (27). Conjugates were measured using the Beckman Coulter Cytoflex. All cytometric data were analyzed using the FlowJo v10.7.

Pulmonary Function Assessment

One week after the transfer of smoke- or air-exposed EVs, mice underwent pulmonary function testing with our flexiVent apparatus (SCIREQ), with methods described previously (27).

Statistical Analyses

All analyses were performed using nonparametric statistics as detailed in the figure legends. Data are expressed as the mean ± SEM, and significance threshold was set as $P = 0.05$.

Results

CS Exposure in Mice Generates Destructive EVs in a Dose-Dependent Manner

We first sought to develop a CS exposure model to comprehensively characterize the contribution of smoking to the emergence of destructive EVs. Accordingly, we exposed cohorts of mice to CS (or ambient air) for increasing durations (1 wk, 2 wk, 1 mo, 3 mo, and 6 mo) (Figure 1A). Over the time course, we observed that the EV numbers were roughly comparable between air- and CS-exposed conditions. The mean size of EVs across all time points was 110.02 ± 5.52 nm in air-exposed conditions and 112.36 ± 4.55 nm in CS-exposed conditions, indicating that a large portion was of exosome size (Figure 1B). To ascertain the pathogenicity of the EVs from CS- and air-exposed mice, we transferredpooled EVs from respective groups intratracheally into the airways of naive A/J mice as described in Figure 1C. After an incubation period of 1 week, the lungs of the mice were analyzed histologically and scored for tissue damage by determining the mean linear intercept (L_m) for each mouse. EVs from CS-exposed mice demonstrated the capacity to elicit alveolar damage in the naive recipients beginning at Week 2 of exposure (Figures 1D and 1E), which is the cusp (2 wk to 1 mo) of onset of airway damage in CS-exposed donor mice (L_m increase of 4 μM CS vs. air [$P < 0.05$] at 1-month exposure) (*see* Figure E2). The pathogenicity of EVs, as measured by the magnitude of L_m change, increased with the length of CS exposure, and the most striking differences in damage were observed at the 6-month time point. The EVs derived from air-exposed mice did not induce damage in the naive recipients and were comparable with those from nontreated control mice, who received saline only. Although we demonstrate that a single dose of CS-exposed EVs is sufficient to prompt damage in naive recipients, we also observed that repeated dosing with EVs over the 1-week study period significantly increased damage in recipients (*see* Figure E3).

One puzzling aspect of our findings was that, at 2 weeks of CS exposure, 10^7 BALF EVs from donors were causing marked alveolar enlargement in naive recipients, whereas there was little, if any, damage in the CS-exposed donors, whose airways contain far more EVs (about 2×10^{10} BALF EVs per mouse) (*see* Figure E4). This suggested that a transient protective mechanism was being activated in the CS-exposed donors that was absent in the naive recipients. This idea was tested by exposing recipient mice to air or CS for 1 or 2 weeks (i.e., before observable CS-mediated damage) and then transferring pathogenic BALF EVs derived from mice exposed to CS for 3 months. We found that after a 1-week exposure, there is a trend

Figure 1. (*Continued*). means of quantifying alveolar enlargement (n = 5 per group). (*E*) Representative images (hematoxylin and eosin) 1 week after EV transfer. Scale bars, 100 μm. (*F*) A/J mice underwent smoke or air exposure for a 1-week or 2-week period. After exposure, mice were treated with one dose of 3-month, smoke-activated EVs (10^7 EVs), and their lung damage was quantified 1 week posttreatment ($n = 4$ or 5 per group). The quantified results are expressed in terms of mean ± SEM. For all comparisons, statistical significance was determined by Mann-Whitney test. *$P < 0.05$ and **$P < 0.01$. ns = not significant.

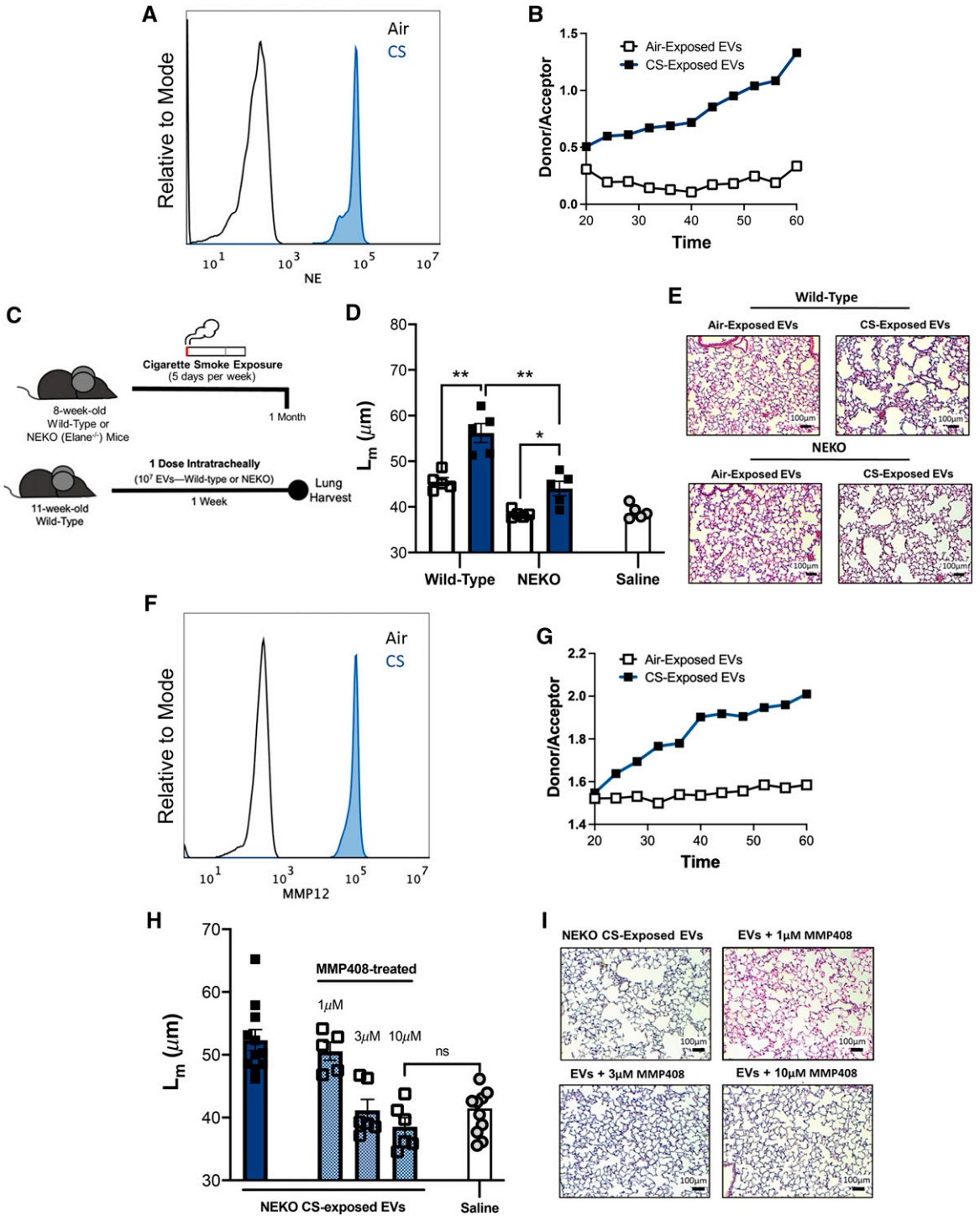

Figure 2. Extracellular vesicle (EV)-driven damage is mediated by neutrophil elastase (NE) and matrix metalloproteinase 12 (MMP12). (*A*) Quantification of EV surface expression of neutrophil elastase (NE) using bead-based flow cytometry. Representative histograms shown are pooled airway EVs acquired from mice exposed to air or cigarette smoking (CS) for 3-months. (*B*) Analysis of NE activity of CS-exposed and air-exposed EVs using a NE-specific fluorescence resonance energy transfer (FRET) assay. Data are representative of 2 or more independent FRET assays. (*C*) Summary of our model of EV acquisition and transfer. Airway EVs from Wild-type or NE-deficient (NEKO) mice receiving cigarette CS for 1 month were harvested, purified, and transferred intratracheally to syngeneic, Wild-type BL/6 mice. Mice were treated with one dose of EVs (10^7) and their lung damage was quantified one-week post-treatment. ($n = 5$ per group). (*D*) Cumulative Mean Linear Intercept (L_m) scoring following transfer of Wild-type or NEKO EVs was determined as a means of quantifying alveolar enlargement. ($n = 5$ per group). (*E*) Representative images (hematoxylin and eosin) one week following EV transfer. Scale bars: 100 μm. (*F*) Quantification of EV surface expression

toward less EV-mediated damage in CS-exposed mice, compared with their air-exposed counterparts (Figure 1F). By 2 weeks, this protection is significant and marked in all CS-exposed mice in comparison with air exposure (Figure 1F). The protection is undoubtedly transient, because all CS-exposed mice eventually succumbed to disease, but this result points to a potentially exciting, new CS-induced protective mechanism that warrants future study and would have been unrecognized in other CS exposure models.

The initial transfer experiments were performed using pooled EV stocks derived from multiple mice. To ensure that the effects that we observed in Figure 1D were not a result of an overcontribution of a single mouse to the EV pool, we next performed individual EV transfers where only the EVs from one donor were used for each recipient (*see* Figure E5). After 3 months of air or CS exposure, we observed that individual transfer of CS-activated EVs still induced notable alveolar enlargement and damage compared with the air-exposed control mice (Figure E5). Moreover, EV-mediated damage from the CS condition was not limited to the A/J mouse strain. We also observed significant damage when transferring CS-activated EVs from the C57BL/6 background to naive, syngeneic recipients (Figure E5). Although histological evidence of tissue destruction is an important disease parameter, we confirmed that mice treated with CS-associated EVs also demonstrated other pathophysiological parameters consistent with alveolar destruction. We found that the mice that receive CS-exposed EVs also exhibited an increase in airway resistance compared with those treated with air-exposed EVs (*see* Figure E6). Of note, a higher dose (10^9) of EVs was necessary to observe changes among the pulmonary function tests. This suggests that, although a lower dose can elicit visible damage in the lungs, a threshold effect exists for the functional changes to be observed. It may also reflect the sensitivity of murine pulmonary function tests to detect early or less advanced disease phenotypes. In addition to the histological and physiological changes observed on treatment with CS-activated EVs, we also observed increases in right ventricular hypertrophy in these mice (Figure E6). This observation not only supports the pulmonary findings in our model but also emphasizes the utility of EV administration as a means to recapitulate the clinical features of COPD and underscores the fidelity of this model to disparate clinical manifestations of COPD.

CS-Activated EVs Drive Lung Damage through NE and MMP12

In light of these observations, we sought to investigate molecular factors associated with EVs that could be driving the pathogenic changes in the lung. To evaluate the mechanism driving the damage and tissue remodeling that we observed in our EV transfer model, we first characterized protease expression on the EV surface using bead-based flow cytometry. Our group, to our knowledge, was the first to demonstrate that EV-bound NE can be found in the airways of individuals with COPD and is capable of inducing tissue damage when transferred to naive mice (3). Moreover, we have demonstrated that NE-bearing EVs are the primary drivers of tissue damage and remodeling associated with acute lung injury induced by lipopolysaccharide (LPS) (27). We first analyzed the cellular composition in the airway after CS exposure. We observed an abundant population of both macrophages and neutrophils at the 1-month and 3-month CS-exposure time points (*see* Figure E7). To determine whether EVs isolated from CS-exposed mice resembled EVs isolated from humans with COPD and EVs from our LPS-exposed mouse model, we measured the surface expression of NE on mouse EVs that had been exposed to CS. We observed that, although air-exposed mice exhibited a low level of expression of the protease, mice that had been exposed to CS for 3 months demonstrated strikingly elevated levels of surface NE (Figure 2A). In addition to increased expression of NE, we observed that the EV fraction from CS-exposed conditions exhibited enhanced NE activity, whereas the EVs from air-exposed mice did not have such activity (Figure 2B).

Given the notable expression and activity of NE associated with CS-activated EVs, we sought to further elucidate the role of this protease in driving EV-induced pulmonary damage. To accomplish this, we first exposed NEKO mice to air or CS for 1 month (Figure 2C). After isolating and purifying the EV fraction from the NEKO mice, we transferred the EVs intratracheally into naive, syngeneic recipients and quantified the EV-mediated damage 1 week later (Figure 2C). The EVs derived from NEKO mice exposed to CS induced less alveolar enlargement relative to EVs derived from CS-exposed wild-type control mice (Figures 2D and 2E). However, the damage from the CS-exposed NEKO conditions was still significant in comparison with air-exposed control mice. This observation was distinct from the findings in our acute LPS model, in which the capacity of EVs to induce alveolar enlargement in recipient animals was completely prevented by the genetic deletion of NE (27). This strongly suggested that another population of EVs might also contribute to the pathogenicity of EVs derived from CS-exposed animals. Moreover, this is similar to our previously published findings using EVs derived from the airways of humans with COPD, in which NE-positive EVs seemed to account for some, but not all, of the alveolar enlargement induced by the total airway EV population (3).

Numerous groups have demonstrated macrophage-derived MMP12 as a critical protease inducing the alveolar damage associated with smoking in humans and in preclinical, animal models of CS exposure (13, 25, 28, 29). The notable concentration of macrophages in the airway after CS exposure (*see* Figure E7) prompted us to measure MMP12 on the surface of airway EVs. Concurrent with the high NE expression, we observed elevated expression of MMP12

Figure 2. (*Continued*). of MMP12 using bead-based flow cytometry. Representative histograms shown are pooled airway EVs acquired from mice exposed to air or CS for 3-months (*G*) Analysis of MMP12 activity of CS-exposed and air-exposed EVs using an MMP12-specific FRET assay. Data are representative of 2 or more independent FRET assays. (*H*) Cumulative L_m scoring following transfer of NEKO EVs was determined as a means of quantifying alveolar enlargement. For some conditions, EVs were pretreated with varying concentrations of an MMP12 inhibitor (MMP408) ($n \geq 5$ per group). (*I*) Representative Images (hematoxylin and eosin) one week following EV transfer. Scale bars, 100 μm. The quantified results are expressed in terms of mean ± SEM. Statistical significance was determined by Mann-Whitney test for all comparisons except in (*H*), where the Kruskal-Wallis test was used. $^{**}P < 0.01$, $^{*}P < 0.05$. ns = not significant.

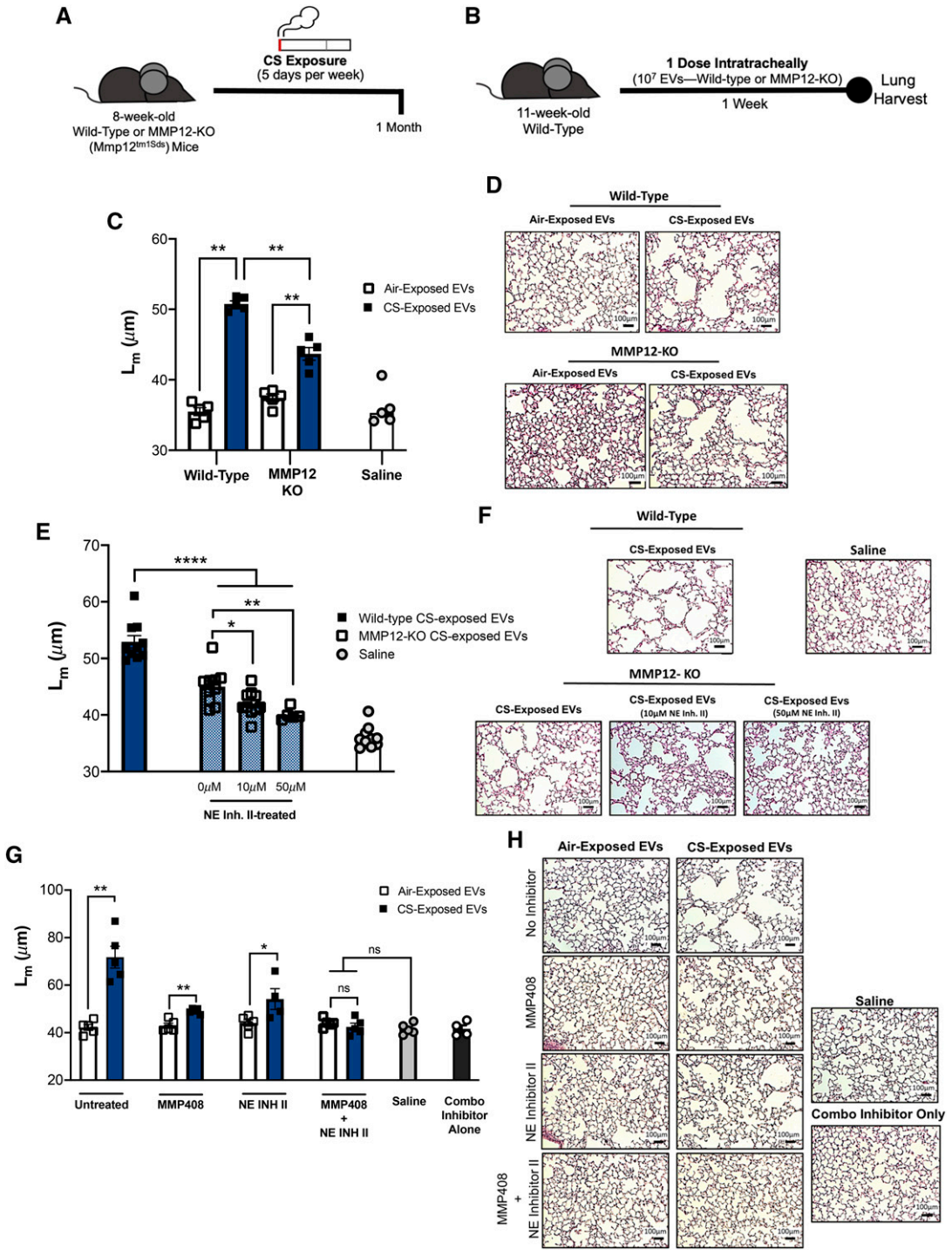

Figure 3. Blockade of matrix metalloproteinase 12 (MMP12) and neutrophil elastase (NE) prevent extracellular vesicle (EV)–mediated lung damage. (*A*) Airway EVs from wild-type or MMP12-deficient (MMP12-KO) mice receiving exposure to cigarette smoking (CS) for 1 month were harvested and purified. (*B*) Mice were treated with one dose (10^7) of wild-type or MMP12-KO EVs, and their lung damage was quantified 1 week posttreatment ($n = 5$ per group). (*C*) Cumulative mean linear intercept (L_m) scoring was determined as a means of quantifying alveolar enlargement ($n = 5$ per group). (*D*) Representative images (hematoxylin and eosin) 1 week after EV transfer. Scale bars, 100 μm. (*E*) Cumulative L_m scoring after transfer of MMP12-KO EVs that were pretreated with varying concentrations of NE Inhibitor II (NE Inh II) ($n = 5$ per group). (*F*) Representative images (hematoxylin and eosin) 1 week after EV transfer. Scale bars, 100 μm. (*G*) Cumulative L_m scoring after the transfer of EVs derived from wild-type mice treated with CS or air for 3 months. In some conditions, EVs were pretreated with MMP408, NE Inh II, or both ($n = 5$ per group). (*H*) Representative images (hematoxylin and eosin) 1 week after EV transfer. Scale bars, 100 μm. The quantified results are expressed in terms of mean ± SEM. Statistical significance was determined by Mann-Whitney test for all comparisons except in (*E*), where the Kruskal-Wallis test was used. $^*P < 0.05$, $^{**}P < 0.01$, and $^{****}P < 0.0001$. ns = not significant.

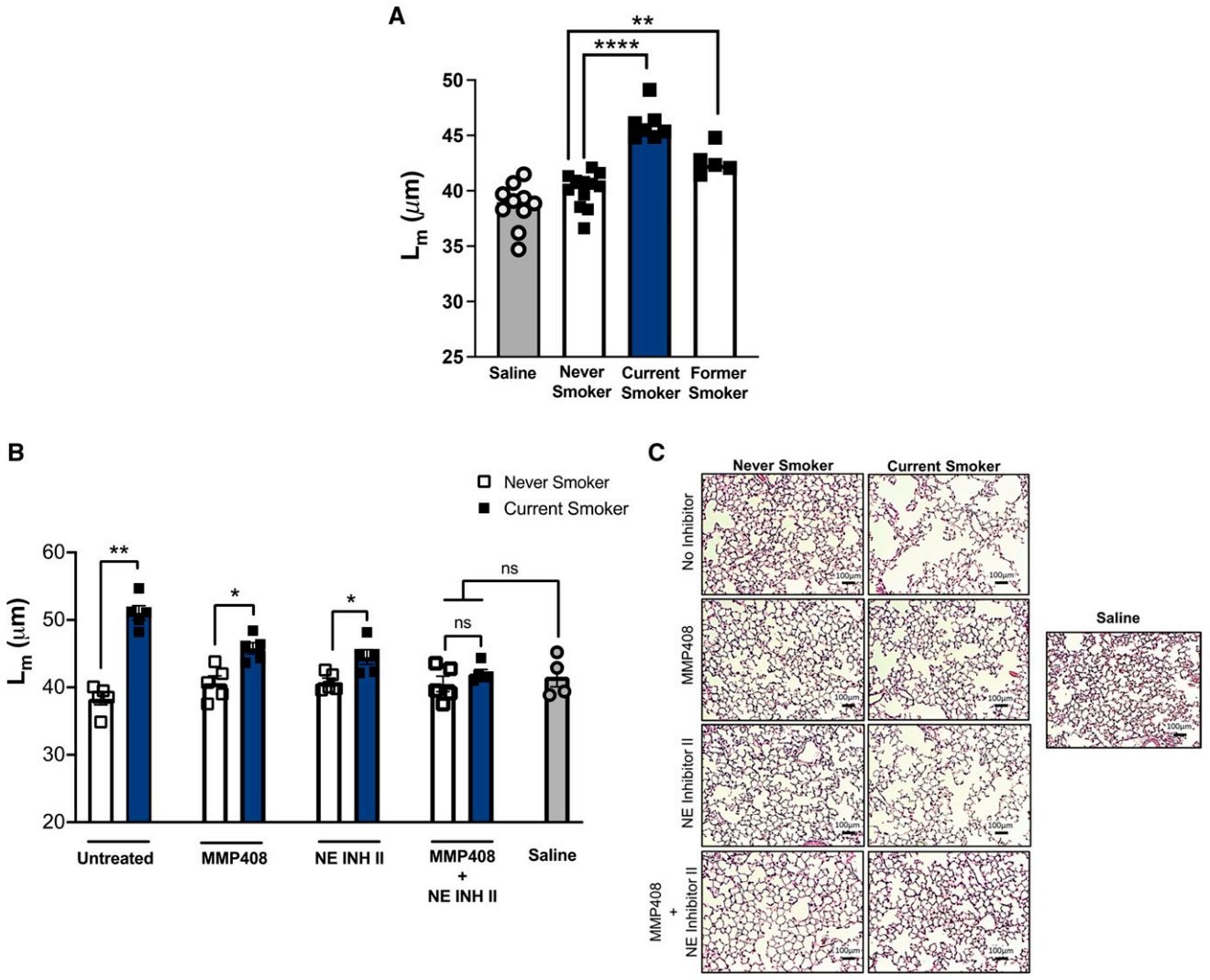

Figure 4. Extracellular vesicles (EVs) from current smokers drive damage through neutrophil elastase (NE) and matrix metalloproteinase 12 (MMP12). Airway EVs from current smokers, former smokers, and never-smokers were harvested and purified from BAL fluid. EVs were delivered intratracheally to naive C57BL/6 mice at a dose of 10^7 EVs per mouse. Lungs were harvested for pathological analyses 1 week posttreatment. (*A*) Cumulative mean linear intercept (L_m) scoring was determined to quantify alveolar damage after treatment with nonpooled human EVs ($n \geq 5$ per group). (*B*) In subsequent experiments, current-smoker and never-smoker EVs were pooled and delivered to naive C57BL/6 mice at a dose of 10^7 EVs per mouse. In some conditions, EVs were pretreated with MMP408, NE Inhibitor II (NE Inh II), or both. Cumulative L_m scoring was determined to quantify alveolar damage ($n = 5$ per group). (*C*) Representative images (hematoxylin and eosin) 1 week after EV transfer. Scale bars, 100 μm. The quantified results are expressed in terms of mean ± SEM. For all comparisons, statistical significance was determined by Mann-Whitney test. $^*P < 0.05$, $^{**}P < 0.01$, and $^{****}P < 0.0001$. ns = not significant.

in EVs from CS-exposed conditions (Figure 2F). This suggested that exposure to CS increases the number of both NE- and MMP12-bearing EVs. Given the expression patterns of MMP12 on the surface of EVs in our model, we assessed MMP12 enzymatic activity of the EV fraction from the BALF. Concurrent with expression, EVs from CS-exposed mice exhibited increased MMP12 enzymatic activity, whereas air-exposed EVs did not (Figure 2G). We next sought to determine whether the EVs bearing MMP12 caused the damage observed in NE-deficient conditions. Using the EVs from mice exposed to CS for 3 months, we measured damage in the NEKO conditions alongside increasing doses of a small molecular weight inhibitor of MMP12 (MMP408). Mice receiving CS-exposed NE-deficient EVs in the absence of MMP408 again exhibited residual alveolar enlargement when compared with mice receiving saline only (Figures 2H and 2I). However, the addition of MMP408 to the CS-activated EVs significantly decreased EV-mediated damage in a dose-dependent manner. In fact, at the higher doses with the inhibitor (3 μM and 10 μM) the L_m scores were not significantly different from those for the saline-only control mice (Figures 2H and 2I). These data indicate that the EV pool generated by smoking relies on both surface-associated NE and MMP12 to aid in the CS-initiated tissue damage.

To confirm the observations made during NE-deficient conditions, we next

repeated similar exposure and treatments on an MMP12-deficient background. We first exposed MMP12-deficient mice (MMP12-KO) to air or CS (Figure 3A). The purified EV fraction was then transferred into naive recipients (Figure 3B). One week after treatment, the lung damage was quantified by L_m scoring. As with NE-deficient conditions, genetic ablation of MMP12 decreased the pathogenicity of the CS-associated EVs compared with wild-type, smoke-exposed mice; however, the damage was still significantly higher than in mice receiving air-exposed EVs (Figures 3C and 3D). To demonstrate any contributing role of NE to the CS-activated EV pool, we next implemented the EV transfer model described in Figures 3A and 3B with varying doses of a small molecular inhibitor of NE (NE Inh II). Although MMP12-KO, CS-exposed EVs still elicit some alveolar damage, CS-activated EVs pretreated with NE Inh II lose their pathogenicity with increasing concentrations of the inhibitor (Figures 3E and 3F).

The observations made in both NE-deficient and MMP12-deficient conditions were also confirmed in wild-type mice using the small–molecular-weight inhibitors. In these experiments, naive mice received EVs from wild-type donors that had been exposed to CS for 3 months. In untreated conditions, as expected, CS-exposed EVs elicited striking damage in the recipients (Figures 3G and 3H). In the single-inhibitor conditions (MMP408 or NE Inh II), CS-associated EV damage was reduced; however, the CS-associated EVs still induced significant damage when compared with the air-exposed EV control mice (Figures 3G and 3H). Only groups that received the combination inhibitor (MMP408 and NE INH II) exhibited L_m scores that were comparable with the scores of air-exposed control mice. These data suggested that both neutrophils and macrophages equally contributed to the pathogenic EV population in the airway. We confirmed this through EV depletion experiments from 3-month CS-exposed mice, which demonstrated that approximately 42.6% of EVs were of neutrophilic origin (Ly6 g^+) and that 37.1% were of macrophage origin ($CD115^+$). A smaller fraction, 5.6%, was of epithelial origin ($EPCAM^+$). Collectively, these studies elucidate a role for both NE- and MMP12-bearing EVs as drivers of alveolar enlargement associated with conventional smoking.

Pathogenic Airway EVs Are Present in Human Smokers and Rely on NE and MMP12 for Activity

To translate our findings from the mouse models, we next investigated whether homologs of the aforementioned mouse EVs were present in the airways of non-COPD human smokers and, if so, whether they required NE and MMP12 for pathogenicity. To accomplish this, we utilized purified EVs from the BALF from current and former smokers, as well as from never-smokers for the control group. Of note, none of these patients had clinical evidence COPD, as our aim was to characterize the effects of CS alone in the absence of COPD. Numerous studies have demonstrated distinct infiltration of both neutrophils and inflammatory macrophages into the airways of smokers (30–33). In our model of EV transfer, we observed that airway EVs from all current smokers, but no never-smokers, caused alveolar enlargement when transferred into mice (Figure 4A). It is interesting that, although the airway EVs from former smokers showed a reduced ability to cause alveolar enlargement, they did not return to the nonpathogenic EV signature associated with never-smokers (Figure 4A). This suggests that, once initiated by CS, the prolonged presence of pathogenic EVs can persist in its absence, perhaps because of the chronic inflammatory environment initiated by CS and propagated by factors such as acrolein and proline-glycine-proline (34).

To ascertain the respective roles of NE and MMP12, we repeated the EV transfer model using the same inhibitor treatment strategy as in our murine model (Figure 3G). We observed, in untreated conditions, that pooled EVs from current smokers elicited robust damage in recipient mice, whereas the EVs from never-smokers did not. When the EVs were pretreated with the single inhibitors (NE Inh II or MMP408), we observed a reduction, but not the elimination, of the capacity of these EVs to induce damage in recipient mice (Figures 4B and 4C). With the combination of inhibitors, however, we observed that the amount of damage was not significantly different from the EVs from never-smokers. These data provide strong support for the observations made in our animal models; moreover, they emphasize both NE and MMP12 as the primary drivers of EV-mediated damage associated with smoking.

Discussion

This study provides new insights into the molecular underpinnings of CS-associated damage in humans and introduces a novel model to study its pathogenesis as well as a newly described CS-induced protective mechanism. A major obstacle for investigators studying the physiological consequences of conventional smoking is the length of time required to generate CS-associated changes in the lung. Using conventional exposure models, it can take months of exposure before alveolar enlargement and lung parenchymal damage can be observed. Our study demonstrates a streamlined method of eliciting the emphysematous changes in recipients in only 1 week. Although traditional methods of CS exposure are required to retrieve the EVs from the airway, the EVs can be cryopreserved, and there is evidence that EVs can be banked for long periods of time (35), thereby circumventing the need for further CS exposure. In addition, EVs from a single mouse are sufficient to cause disease in numerous recipients. This, together with the early tissue remodeling that occurs on EV administration, makes our model an efficient tool for studying the pathogenesis of inflammatory lung diseases, such as COPD.

A remarkable observation from our investigation is how early destructive EVs arise in the context of CS exposure. Exposure to cigarette smoke for only 2 weeks is enough to generate a pathogenic EV signature. Although pathogenicity increases with smoking duration, 2-week CS-activated EVs alone have the capacity to induce emphysematous changes in the lung. These observations suggest that EVs could arise before observable damage can be detected in the CS-exposed donors and warrant more investigation into the potential of these pathogenic entities as predictive biomarkers for COPD and, perhaps, other inflammatory lung diseases.

Our study also highlights the interplay that can exist among different EV populations. Often, in other EVs models, a dominant EV population drives the pathogenic changes. We observed this in

our own model of acute lung injury (27). Our investigations revealed that when LPS is administered to mice as a means to induce lung injury, a major NE-bearing EV fraction arises with the capacity to degrade the lung tissue matrix. The destructive capability of the EVs can be halted on NE blockade (27). In the context of CS exposure, however, there appears to be cooperation among both macrophage- and neutrophil-derived EVs in eliciting the tissue damage associated with CS exposure. Individual blockade of NE or MMP12 (proteases specific to neutrophils and macrophages, respectively) reduces some of the destructive capacity of the CS-associated airway EVs. However, only the inhibition of both proteases is sufficient to neutralize the pathogenicity of the EVs. This highlights the synergy that can exist among distinct EV populations in disease pathogenesis.

A critical and clinically relevant finding from our studies is the observation that disease-driving EVs persist in individuals who have quit smoking. Although the damage prompted by BALF EVs from former smokers is reduced in comparison with that from active smokers, the damage is still significantly elevated compared with findings in never-smokers. It is interesting to speculate that, with extended periods of being smoke free, a subset of former smokers will adopt an EV signature that resembles that of never-smokers and will remain disease-free, whereas pathogenic EVs remain elevated in another subset of former smokers and these individuals will develop COPD. Future longitudinal studies are required to test this idea.

The insights elucidated from the studies described here underscore the role of EVs as initiators of disease processes. In our model, the transfer of the EVs are alone sufficient to prompt both histological and functional changes in the lung and recapitulate clinical features of COPD. Although our study emphasizes pathological changes (i.e., alveolar enlargement), the platform that we have created and its rapid nature will enable the further investigation of multiple facets of CS-associated inflammation. Moreover, the apparent and early role of EVs as drivers of CS-prompted damage highlights them as both potential therapeutic targets and possible predictive biomarkers of COPD. ■

Author disclosures are available with the text of this article at www.atsjournals.org.

Acknowledgment: The authors thank the UAB Comprehensive Flow Cytometry Core for logistical support during the acquisition of the samples included in this study.

References

1. Decramer M, Janssens W, Miravitlles M. Chronic obstructive pulmonary disease. *Lancet* 2012;379:1341–1351.
2. Iheanacho I, Zhang S, King D, Rizzo M, Ismaila AS. Economic burden of chronic obstructive pulmonary disease (COPD): a systematic literature review. *Int J Chron Obstruct Pulmon Dis* 2020;15:439–460.
3. Genschmer KR, Russell DW, Lal C, Szul T, Bratcher PE, Noerager BD, *et al.* Activated PMN exosomes: pathogenic entities causing matrix destruction and disease in the lung. *Cell* 2019;176:113–126.e15.
4. Gon Y, Maruoka S, Inoue T, Kuroda K, Yamagishi K, Kozu Y, *et al.* Selective release of miRNAs via extracellular vesicles is associated with house-dust mite allergen-induced airway inflammation. *Clin Exp Allergy* 2017;47:1586–1598.
5. Russell DW, Genschmer KR, Blalock JE. Extracellular vesicles as central mediators of COPD pathophysiology. *Annu Rev Physiol* 2022;84: 631–654.
6. Salimian J, Mirzaei H, Moridikia A, Harchegani AB, Sahebkar A, Salehi H. Chronic obstructive pulmonary disease: microRNAs and exosomes as new diagnostic and therapeutic biomarkers. *J Res Med Sci* 2018;23:27.
7. Sundar IK, Li D, Rahman I. Small RNA-sequence analysis of plasma-derived extracellular vesicle miRNAs in smokers and patients with chronic obstructive pulmonary disease as circulating biomarkers. *J Extracell Vesicles* 2019;8:1684816.
8. Xie G, Yang H, Peng X, Lin L, Wang J, Lin K, *et al.* Mast cell exosomes can suppress allergic reactions by binding to IgE. *J Allergy Clin Immunol* 2018;141:788–791.
9. Xu H, Ling M, Xue J, Dai X, Sun Q, Chen C, *et al.* Exosomal microRNA-21 derived from bronchial epithelial cells is involved in aberrant epithelium-fibroblast cross-talk in COPD induced by cigarette smoking. *Theranostics* 2018;8:5419–5433.
10. Di Gioia S, Daniello V, Conese M. Extracellular vesicles' role in the pathophysiology and as biomarkers in cystic fibrosis and COPD. *Int J Mol Sci* 2022;24:228.
11. Polverino M, Capuozzo A, Cicchitto G, Ferrigno F, Mauro I, Santoriello C, *et al.* Smoking pattern in men and women: a possible contributor to sex differences in smoke-related lung diseases. *Am J Respir Crit Care Med* 2020;202:1048–1051.
12. Lugg ST, Scott A, Parekh D, Naidu B, Thickett DR. Cigarette smoke exposure and alveolar macrophages: mechanisms for lung disease. *Thorax* 2022;77:94–101.
13. Shapiro SD. The macrophage in chronic obstructive pulmonary disease. *Am J Respir Crit Care Med* 1999;160:S29–S32.
14. Mehta H, Nazzal K, Sadikot RT. Cigarette smoking and innate immunity. *Inflamm Res* 2008;57:497–503.
15. Herrero-Cervera A, Soehnlein O, Kenne E. Neutrophils in chronic inflammatory diseases. *Cell Mol Immunol* 2022;19:177–191.
16. Butler A, Walton GM, Sapey E. Neutrophilic inflammation in the pathogenesis of chronic obstructive pulmonary disease. *COPD* 2018; 15:392–404.
17. Huang G, Xu XC, Zhou JS, Li ZY, Chen HP, Wang Y, *et al.* Neutrophilic inflammation in the immune responses of chronic obstructive pulmonary disease: lessons from animal models. *J Immunol Res* 2017; 2017:7915975.
18. Curtis JL, Freeman CM, Hogg JC. The immunopathogenesis of chronic obstructive pulmonary disease: insights from recent research. *Proc Am Thorac Soc* 2007;4:512–521.
19. Rayner RE, Makena P, Prasad GL, Cormet-Boyaka E. Cigarette and ENDS preparations differentially regulate ion channels and mucociliary clearance in primary normal human bronchial 3D cultures. *Am J Physiol Lung Cell Mol Physiol* 2019;317:L295–L302.
20. Babusyte A, Stravinskaite K, Jeroch J, Lötvall J, Sakalauskas R, Sitkauskiene B. Patterns of airway inflammation and MMP-12 expression in smokers and ex-smokers with COPD. *Respir Res* 2007;8:81.
21. Wells JM, Gaggar A, Blalock JE. MMP generated matrikines. *Matrix Biol* 2015;44–46:122–129.
22. Pandey KC, De S, Mishra PK. Role of proteases in chronic obstructive pulmonary disease. *Front Pharmacol* 2017;8:512.
23. Dey T, Kalita J, Weldon S, Taggart CC. Proteases and their inhibitors in chronic obstructive pulmonary disease. *J Clin Med* 2018;7:244.
24. Gharib SA, Manicone AM, Parks WC. Matrix metalloproteinases in emphysema. *Matrix Biol* 2018;73:34–51.
25. Hautamaki RD, Kobayashi DK, Senior RM, Shapiro SD. Requirement for macrophage elastase for cigarette smoke-induced emphysema in mice. *Science* 1997;277:2002–2004.
26. Churg A, Zhou S, Wright JL. Series "matrix metalloproteinases in lung health and disease": matrix metalloproteinases in COPD. *Eur Respir J* 2012;39:197–209.
27. Margaroli C, Madison MC, Viera L, Russell DW, Gaggar A, Genschmer KR, *et al.* An in vivo model for extracellular vesicle-induced emphysema. *JCI Insight* 2022;7:e153560.

28. Valença SS, da Hora K, Castro P, Moraes VG, Carvalho L, Porto LC. Emphysema and metalloelastase expression in mouse lung induced by cigarette smoke. *Toxicol Pathol* 2004;32:351–356.
29. Churg A, Wang RD, Tai H, Wang X, Xie C, Dai J, *et al.* Macrophage metalloelastase mediates acute cigarette smoke-induced inflammation via tumor necrosis factor-alpha release. *Am J Respir Crit Care Med* 2003;167:1083–1089.
30. Karimi R, Tornling G, Grunewald J, Eklund A, Sköld CM. Cell recovery in bronchoalveolar lavage fluid in smokers is dependent on cumulative smoking history. *PLoS One* 2012;7:e34232.
31. Kuschner WG, D'Alessandro A, Wong H, Blanc PD. Dose-dependent cigarette smoking-related inflammatory responses in healthy adults. *Eur Respir J* 1996;9:1989–1994.
32. Sköld CM, Hed J, Eklund A. Smoking cessation rapidly reduces cell recovery in bronchoalveolar lavage fluid, while alveolar macrophage fluorescence remains high. *Chest* 1992;101:989–995.
33. Lensmar C, Elmberger G, Sandgren P, Sköld CM, Eklund A. Leukocyte counts and macrophage phenotypes in induced sputum and bronchoalveolar lavage fluid from normal subjects. *Eur Respir J* 1998; 12:595–600.
34. Wells JM, O'Reilly PJ, Szul T, Sullivan DI, Handley G, Garrett C, *et al.* An aberrant leukotriene A4 hydrolase-proline-glycine-proline pathway in the pathogenesis of chronic obstructive pulmonary disease. *Am J Respir Crit Care Med* 2014;190:51–61.
35. Jeyaram A, Jay SM. Preservation and storage stability of extracellular vesicles for therapeutic applications. *AAPS J* 2017;20:1.